

# From Static to Dynamic Anomaly Detection with Application to Power System Cyber Security

KAIKAI PAN, PETER PALENSKY, AND PEYMAN MOHAJERIN ESFAHANI

**ABSTRACT.** Developing advanced diagnosis tools to detect cyber attacks is the key to security of power systems. It has been shown that multivariate attacks can bypass bad data detection schemes typically built on static behavior of the systems, which misleads operators to disruptive decisions. In this article, we depart from the existing static viewpoint to develop a diagnosis filter that captures the dynamics signatures of such a multivariate intrusion. To this end, we introduce a dynamic residual generator approach formulated as a robust optimization program in order to detect a class of disruptive multivariate attacks that potentially remain stealthy in view of a static bad data detector. We then reformulate the proposed approach as finite, but possibly non-convex, optimization program. We further develop a linear programming relaxation that improves the scalability, and as such practicality, of the diagnosis filter design. To illustrate the performance of our theoretical results, we implement the proposed diagnosis filter to detect multivariate attacks on the system measurements deployed to generate the so-called Automatic Generation Control signals in a three-area IEEE 39-bus system.

## 1. INTRODUCTION

The digital transformation of our power system does not only lead to better observability, flexibility and efficiency, but also introduces a phenomenon that is new to power system controls: cyber security threats. NIST [7] defines five functions for protecting Information and Communication Technology (ICT): Identify, Protect, Detect, Respond, Recover. It would be naive to think an ICT system can be perfectly protected (point 2) in order to save points 3-5. This paper focuses on point three for supervisory control and data acquisition (SCADA) systems, which are in charge of transmitting measurement and control signals between power system substations and control centers [13], and which are notorious for being based on legacy ICT. Such SCADA systems are a popular target for adversaries [11, 6] nowadays, and it is of utmost importance to detect attacks and respond in an appropriate manner. The consequences of a successful attack to SCADA systems can be catastrophic to an economy and society in general [15]. Notably, if attacks can be detected sufficiently fast, the corrupted signals can be disconnected or corrected by resilient controls, preventing further severe damage [24].

**Literature on Anomaly Detection.** Traditionally, SCADA systems deploy bad data detection (BDD) to filter out possible erroneous measurements due to sensor failures or anomalies [1, 23]. The BDD process captures only a snapshot of the steady states of system trajectories, and thus only exploits possible *static* impact of intrusions. Although this method can perform successfully in detecting basic attacks, it may fail in the presence of the so-called *stealthy attacks* that carefully launch synthesized false data injections [12].

It was first explored in [18] that such an attack can perturb the state estimation function without triggering alarms in BDD. Since then vulnerability and impact analysis of stealthy attacks on power systems have been

---

*Date:* April 22, 2019.

The authors are with the Delft University of Technology, The Netherlands (email: {K.Pan, P.Palensky, P.MohajerinEsfahani}@tudelft.nl).

a prominent subject in the literature. Without advanced diagnosis tools, tampering measurements remains undetected, causing state deviations, equipment damages or even cascading failures [16]. Techniques proposed to deal with stealthy attacks include statistical methods such as sequential detection using Cumulative Sum (CUSUM)-type algorithms [14], and measurements consistency assessment under certain observability assumptions [25]. A detection method that leverages online information is described in [3], which is applicable by ensuring the availability and accuracy of load forecasts and generation schedules. In [17], a mechanism is introduced to formulate the detection scheme as a matrix separation problem, but it only recovers intrusions among corrupted measurements over a particular period of time.

These techniques are essentially static detection methods that may be confined by certain prior assumptions on the distribution of measurement errors. Despite an extensive and ongoing literature focusing on the static part of BDD mechanism, the following question remains largely unexplored:

*Would it be possible to detect stealthy multivariate attacks in a real-time operation by exploiting the attack impact on the dynamics of system trajectories during the transient?*

The importance of an appropriate answer to this question has been reinforced thanks to recent advances in sensing technology in the modern power systems. Our main objective in this article is to address this question.

**Related Work.** Detection methods concerning system dynamics have primarily emerged under the topic of *fault detection and isolation filters*. A subclass of these schemes is the observer-based approach applied initially to linear models [19]; see also [9] for a comprehensive summary of the large body of the literature. The authors in [20] further extend the modeling framework to general linear differential-algebraic equations (DAEs), enhancing the applicability of such methods particularly for power system applications due to the common governing physical laws in this setting. Recently, a variant of observer-based methods is also investigated in [2] so as to deal with unknown natural exogenous inputs.

An inherent shortcoming of observe-based approaches is that the degree of the resulting diagnosis filter is effectively the same as the system dynamics, which may yield an unnecessarily complex filter in large-scale power systems. The closest approach in the literature is [10] where a scalable optimization-based filter design is developed for high-dimensional nonlinear control systems. However, the proposed method opts for mainly dealing with a single fault scenario, and may not be as effective in case of smart multivariate adversarial inputs.

**Our Contributions.** The main objective of this article is to develop a *diagnosis filter* to detect multivariate attacks in a real-time operation. For this purpose, considering a class of disruptive multivariate attack scenarios (Definition 2.5), we first characterize the attack impact on power system dynamics through a set of differential equations. Having transferred the dynamics into the discrete-time domain, we further restrict the diagnosis filter to a family of dynamic residual generators that entirely decouples the contributions of the attacks from the system states and natural disturbances. In order to identify an admissible multivariate attack scenario, we propose an optimization-based framework to robustify the diagnosis filter with respect to such attacks, i.e., aiming to design a filter whose residual (output) is sensitive to any plausible disruptive attacks. The main contributions of this article can be summarized as follows:

- (i) Unlike the existing literature, we go beyond a static viewpoint of anomaly detection to capture the attack impact on the dynamics of system trajectories. To this end, we characterize the diagnosis filter design approach as a robust optimization program. It is guaranteed that while the filter residual is decoupled from system states and disturbances, it still remains sensitive to all admissible disruptive

multivariate attacks even if the attacker has full knowledge about the diagnosis filter architecture (Definition 4.1 and the program (18)).

- (ii) We reformulate the resulting robust program as a finite, possibly non-convex, optimization program (Theorem 4.3). To improve the scalability of the proposed solution, we further propose a linear programming relaxation which is highly tractable for large scale systems (Corollary 4.4). It is guaranteed that if the optimal value of the relaxed program is positive, the resulting diagnosis filter succeeds to detect all admissible disruptive attack scenarios, which may remain stealthy in the lens of a static detector.

In addition to the above theoretical results, we validate the performance and effectiveness of the proposed diagnosis filter on a multi-area IEEE 39-bus system. Numerical results illustrate that the diagnosis filter successfully generates a residual “alert” in the presence of multivariate attacks that are stealthy in a static viewpoint, even in a noisy environment with imprecise measurements.

Section 2 introduces the problem of power system cyber security, and the challenges posed by multivariate attacks are highlighted. Section 3 discusses a model instance of power system dynamics under measurement attacks. Our diagnosis filter design is proposed in Section 4 where an optimization framework is introduced, and numerical simulations are reported in Section 5.

**Notation.** The symbols  $\mathbb{R}$ ,  $\mathbb{R}_+$ ,  $\mathbb{N}$  represent the set of real numbers, nonnegative real numbers, and integers, respectively. Given a matrix  $A \in \mathbb{R}^{m \times n}$ ,  $A^\top$  denotes its transpose, and the space  $\text{Im}(A)$  represents its range space. Throughout the paper, the matrix  $I$  is the identity matrix with an appropriate dimension. Given a column vector  $a \in \mathbb{R}^m$ ,  $\text{diag}(a)$  denotes an  $m \times m$  diagonal matrix with the elements of vector  $a$  sitting on the main diagonal and the rest of the elements being zero. We also denote by  $\text{diag}[A_1, A_2, \dots, A_k]$  a block matrix whose main diagonal elements are the matrices  $A_1, A_2, \dots, A_k$ . Given a vector  $a \in \mathbb{R}^m$ , the associated  $\ell_\infty$ -norm is denoted by  $\|a\|_\infty = \max_{i \leq m} |a_i|$ .

## 2. PROBLEM STATEMENT

### 2.1. Static Detection and System Modeling

For a power grid, measurements are collected by remote sensors and transmitted through a SCADA network. The typical BDD is conducted to detect the erroneous measurements at each time instance. We can see this as a static process: it only concerns the system states  $X[k] \in \mathbb{R}^{n_x}$  and measurements  $Y[k] \in \mathbb{R}^{n_y}$  at time step  $k \in \mathbb{N}$ , which can be described by

$$Y[k] = CX[k] + D_f f[k], \quad (1)$$

where  $C \in \mathbb{R}^{n_y \times n_x}$  is the measurement matrix;  $f[\cdot] \in \mathbb{R}^{n_f}$  denotes the attacks on measurements. Note that the matrix  $D_f$  characterizes which measurement is vulnerable to attacks. It is customary to define a *residual signal* for a static detector,  $r_S[k] := Y[k] - \hat{Y}[k]$ , where  $\hat{Y}[\cdot]$  denotes the estimated measurements. In the traditional weighted least squares estimation, the estimate of state is  $(C^\top C)^{-1} C^\top Y[k]$ , assuming that  $C$  has full column rank with high measurement redundancy. Then the measurements estimate becomes  $C(C^\top C)^{-1} C^\top Y[k]$ , and the residual signal of BDD can be further expressed as

$$r_S[k] = (I - C(C^\top C)^{-1} C^\top) Y[k]. \quad (2)$$

Such an anomaly detector has shown a good effectiveness in detecting erroneous data and basic attacks [8]. However, in the face of coordinated attacks on multiple measurements, this static detector can fail. In this article, motivated by this shortcoming, we take a dynamic design perspective where we shift the emphasis on

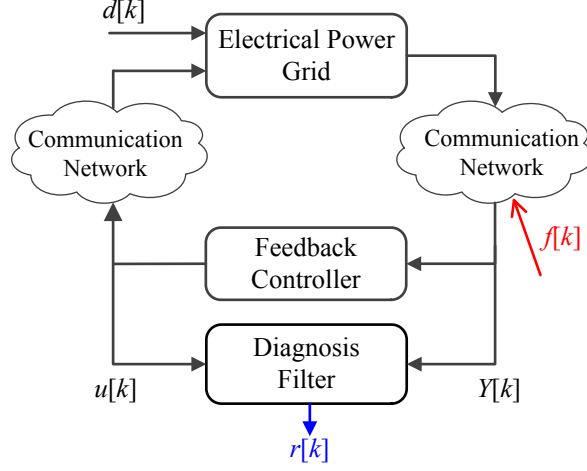


FIGURE 1. Schematic block diagram of the system model.

an attack as a static process to its effects on power system dynamics. In particular, we opt for differentiating the attack impact on the systems trajectories from natural disturbances such as load deviations. To model its impact on the dynamics, let us consider a more general modeling framework in Figure 1. The electrical grid is operated by a digital controller that receives measurements as inputs and sends control signals to the actuators through communication networks. These transmitted data are applied in discrete-time samples. On the power grid side, the input  $d[k] \in \mathbb{R}^{n_d}$  represents natural disturbances. On the controller side, a control signal  $u[k] \in \mathbb{R}^{n_u}$  is computed given the measurements  $Y[k]$ . Note that with the closed-loop control, the corruptions  $f[k]$  on the measurements would affect the system dynamics. A linear description of the closed-loop system is

$$\begin{cases} X[k+1] = A_x X[k] + B_d d[k] + B_u u[k], \\ Y[k] = C X[k] + D_f f[k], \end{cases} \quad (3)$$

where  $A_x$ ,  $B_d$  and  $B_u$  are constant matrices. Note the difference between the dynamic model (3) and the static one (1). To illustrate the attack impact on the system dynamics, we can simply consider the feedback controller as a linear operator such that  $u[k] = G Y[k]$  where  $G \in \mathbb{R}^{n_u \times n_y}$  is a matrix gain. By defining the closed-loop system matrices  $A_{cl} := A + B_u G C$  and  $B_f := B_u G D_f$ , we can reformulate (3) into

$$\begin{cases} X[k+1] = A_{cl} X[k] + B_d d[k] + B_f f[k], \\ Y[k] = C X[k] + D_f f[k]. \end{cases} \quad (4)$$

**Remark 2.1** (Dynamic feedback controller). *The restriction to only a static feedback controller  $u[k] = G Y[k]$  to transfer from (3) to (4) is without loss of generality. Namely, the proposed framework is rich enough to subsume a dynamic controller architecture as well. Indeed, when the controller has certain dynamics, it suffices to augment the system dynamics (3) with the controller states and outputs. We refer to Appendix-B 2.1 for such a detailed analysis.*

**Remark 2.2** (Attacks impact on the dynamics of system trajectories). *In light of (4), matrices  $B_f$ ,  $D_f$  capture the attack impact on the power system dynamics, mapping attacks  $f[\cdot]$  to the system states and measurements respectively.*

In the following, we show that the state-space description (4) is a particular case of DAE model. By introducing a time-shift operator  $q : qX[k] \rightarrow X[k+1]$ , one can fit (4) into

$$H(q)x[k] + L(q)y[k] + F(q)f[k] = 0, \quad (5)$$

where  $x := [X^\top d^\top]^\top$  represents the unknown signals of system states and disturbances;  $y := Y$  contains all the available data for the operator. Let  $n_x$  and  $n_y$  be the dimensions of  $x[\cdot]$ ,  $y[\cdot]$ . We denote  $n_r$  as the number of rows in (5). Then  $H$ ,  $L$ ,  $F$  are polynomial matrices in terms of the time-shift operator  $q$  with  $n_r$  rows and  $n_x, n_y, n_f$  columns separately, by defining,

$$H(q) := \begin{bmatrix} -qI + A_{cl} & B_d \\ C & 0 \end{bmatrix}, \quad L(q) := \begin{bmatrix} 0 \\ -I \end{bmatrix}, \quad F(q) := \begin{bmatrix} B_f \\ D_f \end{bmatrix}.$$

## 2.2. Challenge: Multivariate Attacks

We start this subsection with an existing result characterizing the set of stealthy attacks that can bypass the static detector.

**Lemma 2.3** (Stealthy attack values [18, Theorem 1]). *Consider the measurement equation (1) and the static detector with the respective residual function (2). Then, an attack  $f[\cdot]$  remains stealthy, i.e., it does not cause any additional residue to (2), if it takes values from the set*

$$\mathcal{F} := \{f[k] \in \mathbb{R}^{n_f} : D_f f[k] \in \text{Im}(C), \quad k \in \mathbb{N}\}, \quad (6)$$

One can observe that a stealthy attack  $D_f f[\cdot]$  indeed lies in the range space of  $C$  that represents a tampered value  $D_f f[k] = C\Delta X$  where  $\Delta X \in \mathbb{R}^{n_x}$  can be any injected bias influencing certain sensor measurements. Such multivariate attacks would challenge the detector design as they may neutralize the diagnosis filter outputs.

**Assumption 2.4** (Stationary attacks). *Throughout this article, we consider attacks  $f[\cdot]$  that are time-invariant, i.e.,  $f[k] = 0$  for all  $k \leq k_{\min}$ ;  $f[k] = f \in \mathcal{F}$  for all  $k > k_{\min}$ . Namely, the attack occurs as a constant bias injection  $f$  on measurements during the system operations at a specific unknown time instance  $k_{\min}$ , and it remains unchanged since then.*

Advanced attacks also pursue a maximized impact on the system dynamics. Thus, an adversary would try to inject “smart” false data, possibly with large magnitudes, in such a way that it causes the maximum damage. The next definition opts to formalize this class of attacks.

**Definition 2.5** (Disruptive stealthy attack). *Consider a set of vectors  $F_b := [f_1, f_2, \dots, f_d]$  representing a finite basis for the set of stealthy attacks (6), i.e., the set  $\mathcal{F}$  defined in (6) can equivalently be represented by*

$$\mathcal{F} = \left\{ F_b^\top \alpha = \sum_{i=1}^d \alpha_i f_i \mid \alpha = [\alpha_1, \alpha_2, \dots, \alpha_d]^\top \in \mathbb{R}^d \right\}.$$

We call a signal  $f \in \mathcal{F}$  disruptive stealthy attack if its corresponding coefficients  $\alpha$  is a polytopic set, i.e., it belongs to

$$\mathcal{A} := \{\alpha \in \mathbb{R}^d \mid A\alpha \geq b\}, \quad (7)$$

where  $A \in \mathbb{R}^{n_b \times d}$  and  $b \in \mathbb{R}^{n_b}$  are given matrices. We emphasize that the subsequent analysis and the proposed diagnosis filter design only rely on the convexity of the set  $\mathcal{A}$ . Namely, the choice (7) may be adjusted according to the application at hand, as long as the convexity of the set is respected.

## 3. CYBER SECURITY OF POWER SYSTEMS: AGC MODELING

In this section, we first go through a modeling instance of power system dynamics in the form of (4): AGC closed-loop system under attacks. This model will be used to validate our diagnosis filter. Figure 2 depicts the diagram of a three-area IEEE 39-bus system. AGC is a feedback controller that tunes the setpoints of

participated generators (e.g., G11 of Area 1) to maintain the frequency as its nominal value and the tie-line (e.g., L1-2 between Area 1 and 2) power as the scheduled one.

In the work of AGC, a linearized model is commonly used for the load-generation dynamics [22]. For a multi-area system, the frequency dynamics in Area  $i$  can be written as

$$\Delta\dot{\omega}_i = \frac{1}{2H_i}(\Delta P_{m_i} - \Delta P_{tie_i} - \Delta P_{l_i} - D_i\Delta\omega_i), \quad (8a)$$

where  $H_i$  is the equivalent inertia constant;  $D_i$  is the damping coefficient and  $\Delta P_{l_i}$  denotes load deviations. Here  $\Delta P_{tie_i}$ ,  $\Delta P_{m_i}$  represent the total tie-line power exchanges from Area  $i$  and the total generated power in Area  $i$ , i.e.,  $\Delta P_{tie_i} = \sum_{j \in \mathcal{E}_i} \Delta P_{tie_{i,j}}$  where  $\mathcal{E}_i$  denotes the set of areas that connect to Area  $i$ , and  $\Delta P_{m_i} = \sum_{g=1}^{G_i} \Delta P_{m_{i,g}}$  where  $G_i$  denotes the number of participated generators in Area  $i$ , and we have

$$\Delta\dot{P}_{m_{i,g}} = -\frac{1}{T_{ch_{i,g}}}(\Delta P_{m_{i,g}} + \frac{1}{S_{i,g}}\Delta\omega_i - \phi_{i,g}\Delta P_{agc_i}), \quad (8b)$$

$$\Delta\dot{P}_{tie_{i,j}} = T_{ij}(\Delta\omega_i - \Delta\omega_j), \quad (8c)$$

where  $T_{ch_{i,g}}$  is the governor-turbine's time constant;  $S_{i,g}$  denote the droop coefficient;  $T_{ij}$  is the synchronizing parameter between Area  $i$  and  $j$ . Note that  $\Delta P_{agc_i}$  is the signal from AGC for the participated generators to track the load changes, and  $\phi_{i,g}$  is the participating factor, i.e.,  $\sum_{g=1}^{G_i} \phi_{i,g} = 1$ . After receiving the frequency and tie-line power measurements, the *area control error* (ACE) is computed for an integral action,

$$ACE_i = B_i\Delta\omega_i + \sum_{j \in \mathcal{E}_i} \Delta P_{tie_{i,j}}, \quad (8d)$$

$$\Delta\dot{P}_{agc_i} = -K_{I_i}ACE_i, \quad (8e)$$

where  $B_i$  is the frequency bias and  $K_{I_i}$  represents the integral gain. Based on the equations (8), the linearized model of Area  $i$  can be presented as the state equation

$$\dot{X}_i(t) = A_{ii}X_i(t) + B_{i,d}d_i(t) + \sum_{j \in \mathcal{E}_i} A_{ij}X_j(t), \quad (9)$$

where  $X_i$  is the state vector;  $d_i := \Delta P_{l_i}$  denotes load deviations. Recall Remark 2.1 that (9) is an augmented model for the closed-loop AGC system that  $X_i$  consists of not only the electrical grid states (e.g., frequency, generator output and tie-line power) but also the controller state  $\Delta P_{agc_i}$ , i.e.,

$$X_i := \left[ \{\Delta P_{tie_{i,j}}\}_{j \in \mathcal{E}_i} \quad \Delta\omega_i \quad \{\Delta P_{m_{i,g}}\}_{1:G_i} \quad \Delta P_{agc_i} \right]^\top.$$

Besides in (9),  $A_{ii}$  is the system matrix of Area  $i$ ;  $A_{ij}$  is a matrix whose only non-zero element is  $-T_{ij}$  in row 1 or 2 and column 3;  $B_{i,d}$  is the matrix for load deviations.

In addition to (9), we assume a measurement model with high redundancy that the measurements of each tie-line power ( $\Delta P_{tie_{i,j}}$ ) and the total tie-lines' power ( $\Delta P_{tie_i}$ ), the frequency ( $\Delta\omega_i$ ), each generator output ( $\Delta P_{m_{i,g}}$ ) and the total generated power ( $\Delta P_{m_i}$ ), and the AGC controller output ( $\Delta P_{agc_i}$ ) are all available. Besides, vulnerabilities within SCADA networks may allow cyber intrusions. Thus the output equation is

$$Y_i(t) = C_iX_i(t) + D_{i,f}f_i(t), \quad (10)$$

where  $Y_i$  is the system output and  $C_i$  is the output tall-matrix with full column rank. Here  $f_i$  denotes multivariate attacks and the matrix  $D_{i,f}$  quantifies which output is attacked. In the aforementioned section, due to the feedback loop, attacks on the measurements would also affect the frequency dynamics. Hence the state equation (9) during attacks becomes

$$\dot{X}_i(t) = A_{ii}X_i(t) + B_{i,d}d_i(t) + B_{i,f}f_i(t) + \sum_{j \in \mathcal{E}_i} A_{ij}X_j(t),$$

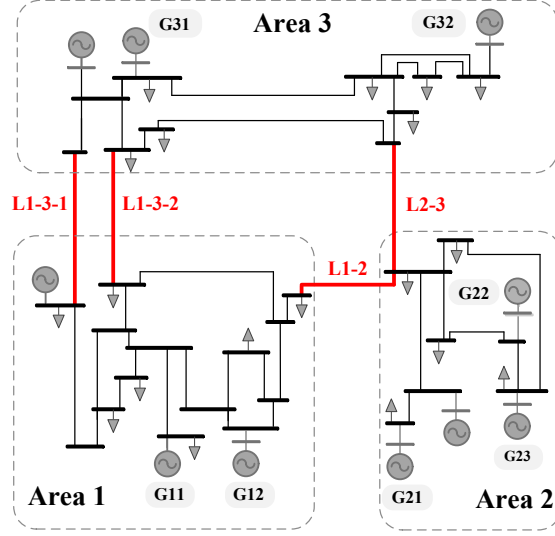


FIGURE 2. Three-area 39-bus system: the measurements of the tie-lines (in red) L1-3, L1-2, L2-3 are attacked.

where  $B_{i,f}$  is the matrix that relates attacks to system states. Using the state equations of each area, the continuous-time model of the three-area system can be obtained,

$$\dot{X}(t) = \tilde{A}_{cl}X(t) + \tilde{B}_d d(t) + \tilde{B}_f f(t), \quad (11)$$

where  $X$  is the vector consisting of groups of dynamic states in each area;  $d$  is the vector for all areas' load deviations;  $f$  denotes all the attack signals in the three-area, namely,

$$X = \begin{bmatrix} X_1^\top & X_2^\top & X_3^\top \end{bmatrix}^\top, \\ d = \begin{bmatrix} \Delta P_{l_1} & \Delta P_{l_2} & \Delta P_{l_3} \end{bmatrix}^\top, \quad f = \begin{bmatrix} f_1^\top & f_2^\top & f_3^\top \end{bmatrix}^\top.$$

In (11),  $\tilde{A}_{cl}$  is the closed-loop system matrix;  $\tilde{B}_d$ ,  $\tilde{B}_f$  are constant matrices that relate load deviations and attacks to system states. For the three-area system, these matrices are

$$\tilde{A}_{cl} = \begin{bmatrix} A_{11} & A_{12} & A_{13} \\ A_{21} & A_{22} & A_{23} \\ A_{31} & A_{32} & A_{33} \end{bmatrix}, \\ \tilde{B}_d = \text{diag} [B_{1,d}, B_{2,d}, B_{3,d}], \quad \tilde{B}_f = \text{diag} [B_{1,f}, B_{2,f}, B_{3,f}].$$

We can also obtain the output equation of the system,

$$Y(t) = CX(t) + D_f f(t), \quad (12)$$

where  $Y$  is the system output vector containing all the three areas' outputs;  $C$  is the output matrix;  $D_f$  quantifies all the vulnerable signals. Similarly, these matrices are

$$Y = \begin{bmatrix} Y_1^\top & Y_2^\top & Y_3^\top \end{bmatrix}^\top, \\ C = \text{diag} [C_1, C_2, C_3], \quad D_f = \text{diag} [D_{1,f}, D_{2,f}, D_{3,f}].$$

To obtain the sampled discrete-time model as (4), (11) and (12) must be discretized. We deploy a zero-order hold (ZOH)<sup>1</sup> discretization for a given sampling period  $T_s$  [21],

$$A_{cl} = e^{\tilde{A}_{cl}T_s}, \quad B_d = \int_0^{T_s} e^{\tilde{A}_{cl}(T_s-t)} \tilde{B}_d dt. \quad (13)$$

Note that the attack matrix  $\tilde{B}_f$  has the same matrix transformation as  $\tilde{B}_d$ , resulting  $B_f$ . The above approximation is exact for a ZOH and (13) corresponds to the analytical solution of the discretization. Therefore, the above model can be described in the form of (4) which again can be fitted into the DAE (5). In Appendix B.2.2 we provide the detailed description of the parameters and matrices in the three-area 39-bus system under cyber attacks on AGC.

#### 4. ROBUST DYNAMIC DETECTION

##### 4.1. Preliminaries for Diagnosis Filter Construction

An ideal detection aims to implement a non-zero mapping from the attack to the diagnostic signal while decoupled from system states and disturbances, given the available data  $y[\cdot]$  in the control center. In the power system dynamics described via a set of DAE, we restrict the diagnosis filter to a type of dynamic residual generator in the form of linear transfer functions, i.e.,  $r_D[k] := R(q)y[k]$  where  $r_D$  is the residual signal of the diagnosis filter and  $R(q)$  is a transfer operator. Note that  $y[\cdot]$  is associated with the polynomial matrix  $L(q)$  in (5). We propose a formulation of transform operator  $R(q)$  as

$$R(q) := a(q)^{-1}N(q)L(q),$$

where  $N(q)$  is a polynomial vector with the dimension of  $n_r$  and a predefined order  $d_N$ . To make  $R(q)$  physically realizable, stable dynamics  $a(q)$  with sufficient order need to be added as the denominator where all the roots are strictly contained in the unit circle. Note that, unlike the observer-based methods, here  $d_N$  can be much less than the dimension of system dynamics. Then  $N(q)$  and  $a(q)$  are the two variables for a diagnosis filter design. By multiplying  $a(q)^{-1}N(q)$  in the left of (5), we have

$$\begin{aligned} r_D[k] &= a(q)^{-1}N(q)L(q)y[k] \\ &= -\underbrace{a(q)^{-1}N(q)H(q)x[k]}_{(I)} - \underbrace{a(q)^{-1}N(q)F(q)f[k]}_{(II)}, \end{aligned} \quad (14)$$

where term (I) in (14) is due to  $x[\cdot]$  of system states and natural disturbances. Term (II) is the desired contribution from the attacks  $f[\cdot]$ . In view of this diagnosis filter description, we introduce a class of residual generator which is sensitive to disruptive stealthy attacks as defined in Definition 2.5.

**Definition 4.1** (Robust residual generator). *Consider a linear residual generator represented via a polynomial vector  $N(q)$ . This residual generator is robust with respect to disruptive stealthy attacks introduced in Definition 2.5 if*

$$\begin{cases} (I) & N(q)H(q) = 0, \\ (II) & N(q)F(q)F_b\alpha \neq 0, \quad \text{for all } \alpha \in \mathcal{A}, \end{cases} \quad (15)$$

where the basis matrix  $F_b$  and the set  $\mathcal{A}$  are the same as the ones in Definition 2.5.

In the next step, we show that the polynomial equations (15) in Definition 4.1 can be characterized as a feasibility problem of a finite robust program.

<sup>1</sup>The inputs signals  $d(\cdot)$  and  $f(\cdot)$  in (11) are assumed to be piecewise constant within the sampling periods.



**Lemma 4.2** (Linear program characterization). *Consider the polynomial matrices  $H(q) = \sum_{i=0}^1 H_i q^i$ ,  $N(q) := \sum_{i=0}^{d_N} N_i q^i$  and  $F(q) = F$ , where  $H_i \in \mathbb{R}^{n_r \times n_x}$ ,  $N_i \in \mathbb{R}^{n_r}$ , and  $F \in \mathbb{R}^{n_r \times n_f}$  are constant matrices. Then, the family of robust residual generators in (15) is characterized by*

$$\begin{cases} (I) & \bar{N}\bar{H} = 0, \\ (II) & \|\bar{N}V(\alpha)\|_\infty > 0, \quad \text{for all } \alpha \in \mathcal{A}, \end{cases} \quad (16)$$

where  $\|\cdot\|_\infty$  denotes the infinite vector norm, and

$$\begin{aligned} \bar{N} &:= \begin{bmatrix} N_0 & N_1 & \cdots & N_{d_N} \end{bmatrix}, \\ \bar{H} &:= \begin{bmatrix} H_0 & H_1 & 0 & \cdots & 0 \\ 0 & H_0 & H_1 & 0 & \vdots \\ \vdots & 0 & \ddots & \ddots & 0 \\ 0 & \cdots & 0 & H_0 & H_1 \end{bmatrix}, \\ V(\alpha) &:= \begin{bmatrix} FF_b\alpha & 0 & \cdots & 0 \\ 0 & FF_b\alpha & 0 & \vdots \\ \vdots & 0 & \ddots & 0 \\ 0 & \cdots & 0 & FF_b\alpha \end{bmatrix}. \end{aligned}$$

*Proof.* The proof follows a similar line of arguments as [10, Lemma 4.2]. The key step is to observe that  $N(q)H(q) = \bar{N}\bar{H}[I, qI, \dots, q^{d_N+1}I]^\top$ , and  $N(q)FF_b\alpha = \bar{N}V(\alpha)[I, qI, \dots, q^{d_N}I]^\top$ . The rest of the proof follows rather straightforwardly, and we omit the details for brevity.  $\square$

## 4.2. Maximin Optimization-based Diagnosis Filter

In light of (16), we can define a symmetric set for the design variable  $\bar{N}$  of the dynamic residual generator,

$$\mathcal{N} := \{\bar{N} \in \mathbb{R}^{(d_N+1)n_r} \mid \bar{N}\bar{H} = 0, \|\bar{N}\|_\infty \leq \eta\}. \quad (17)$$

The second constraint in the set is added to avoid possible unbounded solutions. To design a robust residual generator, we aim to find an  $\bar{N} \in \mathcal{N}$  that for all  $\alpha \in \mathcal{A}$ , (16) can be satisfied. To this end, a natural reformulation of the residual synthesis is to consider an objective function as the second quantity in (16) influenced by the parameters  $\mathcal{N}$  and the attacker action  $\alpha$ , i.e.,  $\mathcal{J}(\bar{N}, \alpha) := \|\bar{N}V(\alpha)\|_\infty$ . A successful scenario from an attacker viewpoint is to minimize this objective function given a residual generator. Therefore, we take a rather conservative viewpoint where the attacker may have knowledge about the residual generator parameters and exploits it so as to synthesize a stealthy attack. We then reformulate the diagnosis filter design as the robust optimization program,

$$\gamma^* := \max_{\bar{N} \in \mathcal{N}} \min_{\alpha \in \mathcal{A}} \left\{ \mathcal{J}(\bar{N}, \alpha) := \|\bar{N}V(\alpha)\|_\infty \right\}. \quad (18)$$

The optimal value  $\gamma^*$  of the robust reformulation (18) is indeed an indication whether the attack still remains stealthy in the dynamic setting, i.e., if  $\gamma^* > 0$  then the optimal solution  $\bar{N}^*$  helps construct a diagnosis filter in the form of (14) which detects all the admissible attacks introduced in Definition 2.5. However, if  $\gamma^* = 0$ , then it implies that for any possible detectors (static or dynamic) there exists a stationary disruptive attack that remains stealthy. In the next step, we show that the robust program (18) can be equivalently reformulated as a finite (non-convex) optimization problem.

**Theorem 4.3** (Finite reformulation of robust design). *The robust optimization (18) can be equivalently described via the finite optimization program*

$$\begin{aligned} \gamma^* &= \max_{\bar{N}, \beta, \lambda} b^\top \lambda \\ \text{s.t.} \quad & \sum_{i=0}^{d_N} (\beta_{2i} - \beta_{2i+1}) N_i F F_b = \lambda^\top A, \\ & \mathbf{1}^\top \beta = 1, \beta \geq 0, \\ & \bar{N} \in \mathcal{N}, \lambda \geq 0. \end{aligned} \tag{19}$$

where  $\beta = [\beta_0, \beta_1, \dots, \beta_{2d_N+1}]^\top$  is an  $\mathbb{R}^{2d_N+2}$ -valued auxiliary variable.

*Proof.* See Appendix-A. □

The exact reformulation program (19) for (18) is unfortunately non-convex due to the bilinearity between the variables  $\beta$  and  $N_i$  in the first constraint. In the following corollary, we suggest a convex relaxation of the program by restricting the feasible set of the variable  $\beta$  to a  $2d_N + 2$  finite possibilities where  $\beta = [0, \dots, 1, \dots, 0]^\top$  in which the only non-zero element of the vector is the  $i^{\text{th}}$  element.

**Corollary 4.4** (Linear program relaxation). *Given  $i \in \{1, \dots, 2d_N + 2\}$ , consider the linear program*

$$\begin{aligned} \gamma'_i &:= \max_{\bar{N}, \lambda} b^\top \lambda \\ \text{s.t.} \quad & (-1)^i N_{\lfloor i/2 \rfloor} F F_b = \lambda^\top A, \\ & \bar{N} \in \mathcal{N}, \lambda \geq 0, \end{aligned} \tag{LP}_i$$

where  $\lfloor \cdot \rfloor$  is the ceiling function that maps the argument to the least integer. Then, the solution to the program (LP<sub>*i*</sub>) is a feasible solution to the exact robust design reformulation (19), and  $\max_{\{i \leq 2d_N+2\}} \gamma'_i \leq \gamma^*$ . In particular, if for any  $i \in \{1, \dots, 2d_N + 2\}$  we have  $\gamma'_i > 0$ , then the solution to LP<sub>*i*</sub> offers a robust residual generator detecting all admissible disruptive attacks introduced by Definition 2.5.

Corollary 4.4 suggests that the maximum optimal value of  $\{\gamma'_0, \gamma'_1, \dots, \gamma'_{2d_N+2}\}$  and the corresponding  $\bar{N}^*$  provide a suboptimal solution to the original robust design (18).

The proposed robust design does not necessarily enforce a non-zero steady-state residual of the diagnosis filter under multivariate attacks. Indeed, the residual signal  $r_D$  may become zero again after a successful diagnosis in a transient behavior. A more stringent perspective is to require a non-zero steady-state behavior under any plausible attack scenario in  $\alpha \in \mathcal{A}$ . This is addressed in the next remark.

**Remark 4.5** (Non-zero steady-state residual). *In order to design a diagnosis filter with non-zero steady-state residual “alert” when a multivariate attack occurs, the robust optimization (18) can be modified by a more conservative (smaller) objective function  $\mathcal{J}(\bar{N}, \alpha) := |\bar{N} \bar{F} \alpha|$  where  $\bar{F} := [F F_b \quad F F_b \quad \dots \quad F F_b]^\top$ . A similar treatment as the one mentioned in Theorem 4.3 and the relaxation in Corollary 4.4 may be deployed for numerical purposes. We refer to Appendix-C for further details along this direction.*

## 5. NUMERICAL RESULTS

### 5.1. Test System And Diagnosis Filter Description

In order to validate the effectiveness of the diagnosis filter with application to power system cyber security, we employed the IEEE 39-bus system which is well-known as a standard system for testing of new power

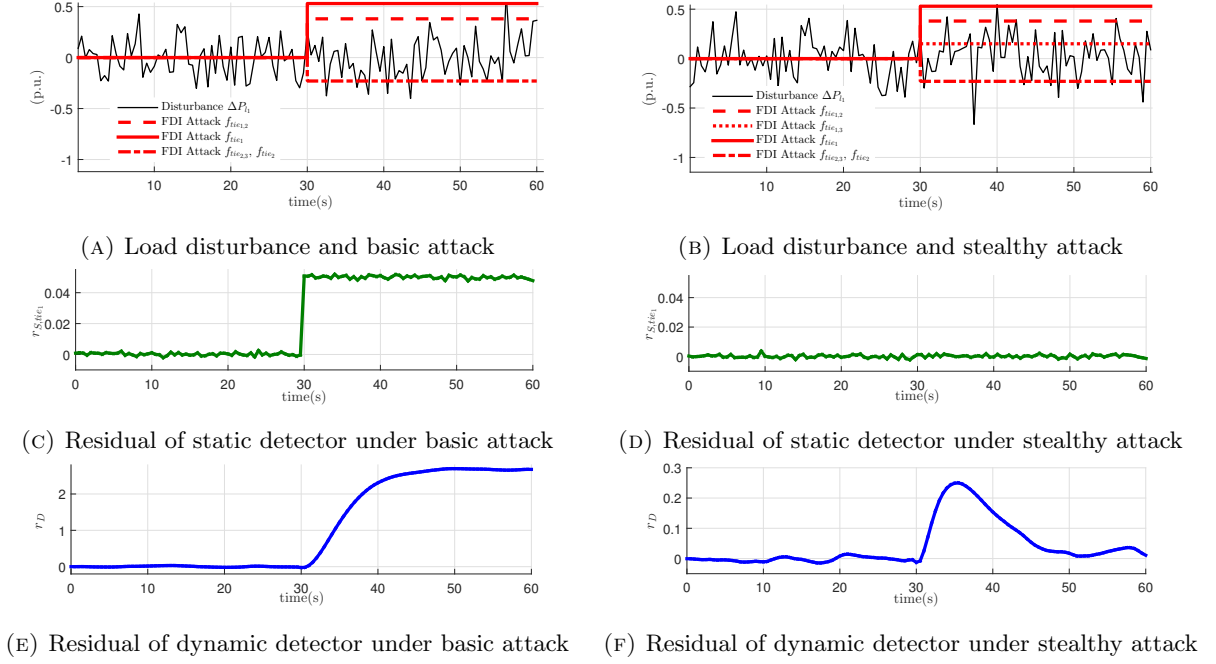


FIGURE 3. Static detector in (2) versus dynamic detector (diagnosis filter) from Corollary 4.4 under basic and stealthy attacks.

system analysis. As shown in Figure 2, this system consists of 3 areas and 10 generators where 7 of them are equipped with AGC for frequency control. All the participating generators in each area are with equal participation factors. The total load of the three-area system is 5.483 GW for the base of 100 MVA and 60 Hz. The generator specifications and AGC parameters of each area are referred to [4], and the linear frequency dynamics model has been developed in the preceding Section 3. Thus we result in a 19-order model in the form of (4).

We apply the diagnosis filter proposed in Section 4 to detect multivariate disruptive attacks on the measurements of AGC system. In the following simulations, we set the degree of the dynamic residual generator  $d_N = 3$  which is much less than the order of the dynamics model, the sampling time  $T_s = 0.5$  sec and the finite time horizon 60 sec. To design the filter, we set the denominator in the form  $a(q) = (q-p)^{d_N} / (1-p)^{d_N}$  where  $p$  is a user-defined variable acting as the *pole* of the transfer operator  $R(q)$ , and it is normalized in steady-state value for all feasible poles. The pole is fixed to be  $p = 0.8$  for a stable dynamic behaviour, and we have deployed the solver CPLEX to solve the corresponding optimization problems.

## 5.2. Simulation Results

To evaluate the performance of the diagnosis filter, the disturbances  $d_i = \Delta P_{l_i}$  are modeled as stochastic load patterns. To capture its uncertainty, as shown in Figure 3a and Figure 3b, we mainly model  $\Delta P_{l_1}$  in Area 1 as random zero-mean Gaussian signals. It should be noted that tie-line power flow measurements are much more vulnerable to cyber attacks, comparing with frequency measurements (e.g., the anomalies in frequency can be easily detected by comparing the corrupted reading with the normal one.) [5]. Therefore as indicated in Figure 2 we mainly focus on the scenario that there are 5 vulnerable tie-line power measurements, namely  $\Delta P_{tie1,2}$ ,  $\Delta P_{tie1,3}$ ,  $\Delta P_{tie1}$ ,  $\Delta P_{tie2,3}$  and  $\Delta P_{tie2}$ . Recalling Definition 2.5 for stealthy attack basis, thus there exist 3 basis vectors in the spanning set and we model them as follows:  $f_1 = [0.1 \ 0 \ 0.1 \ 0 \ 0]^T$ ,

$f_2 = [0.1 \ 0.15 \ 0.25 \ 0 \ 0]^T$ ,  $f_3 = [0 \ 0 \ 0 \ 0.1 \ 0.1]^T$  (all in p.u.). Here each basis vector lies in the range space of the output matrix that the corrupted measurements still align with an actual physical state, bypassing the static detector  $r_S[\cdot]$ . Furthermore, without loss of generality we set  $A = \mathbf{1}^\top$  and  $b = 1.5$  in the set  $\mathcal{A}$  and  $\eta = 10$  in the set  $\mathcal{N}$ . The design variable  $\bar{N}$  of the robust residual generator is derived by solving (18) through (LP<sub>*i*</sub>). The optimal value achieves maximum for  $i = 2$  that  $\gamma'_2 = 300$ , which implies a robust detection as Corollary 4.4. For the given  $\bar{N}$ , the multivariate attack coordinates  $\alpha = [2.8 \ 1 \ -2.3]^\top$  is obtained by solving the inner minimization of (18).

In the first simulation, we begin with a general scenario where the multivariate attack is not carefully coordinated, i.e., basic attack. Thus as shown in Figure 3a, only 4 of 5 vulnerable measurements are compromised that  $f_{tie_{1,2}} = 0.38p.u.$ ,  $f_{tie_1} = 0.53p.u.$ ,  $f_{tie_{2,3}} = -0.23p.u.$  and  $f_{tie_2} = -0.23p.u.$ . Note that since the injected data on  $\Delta P_{tie_{1,2}}$  and  $\Delta P_{tie_1}$  are inconsistent, the static detector is also expected to be triggered. To test the detectors in a more realistic setup, we also consider the presence of process and measurements noises. The process noise term added to the state equation of Area 1 is zero-mean Gaussian noises with the covariance matrix  $R_{X_1} = 0.03 \times \text{diag}([1 \ 1 \ 0.03 \ 1 \ 1 \ 1]^\top)$ , i.e., the covariance of the noise to the frequency is 0.009 and the covariance of other states' noise is 0.03 [2]. Similarly, the measurement noise term added to the measurements of Area 1 is with the covariance matrix  $R_{Y_1} = 0.03 \times \text{diag}([1 \ 1 \ 1 \ 0.03 \ 1 \ 1 \ 1 \ 1]^\top)$ , i.e., the covariance of the frequency measurement is 0.009 and the covariance of other measurements' noise is 0.03 [2]. Note the residue  $r_S$  of BDD in (2) becomes  $r_S[k] = (I - C(C^\top R_Y^{-1} C)^{-1} C^\top R_Y^{-1}) Y[k]$  under the noisy system. The attacks are launched at  $k_{\min} = 30$  sec. In Figure 3c and Figure 3e, results of the static detector in (2) and the proposed dynamic detector (diagnosis filter) are presented. In Figure 4 of Appendix B 2.3, we also present the simulation results under ideal scenarios where there is no noise in the process and measurements. Both detectors have succeeded to generate a diagnostic signal when attacks occurred, and the diagnosis filter residual  $r_D$  is significantly decoupled from stochastic load disturbances, and keeps sensitive to the multivariate attacks for a successful detection under noisy system settings.

In the second simulation, to challenge the detectors, now the multivariate attacks have been launched on all the 5 vulnerable measurements and the derived attack coefficient  $\alpha$  from the optimization results has been used for a more intelligent adversary. Thus in Figure 3b, the corruptions become  $f_{tie_{1,2}} = 0.38p.u.$ ,  $f_{tie_{1,3}} = 0.15p.u.$ ,  $f_{tie_1} = 0.53p.u.$ ,  $f_{tie_{2,3}} = -0.23p.u.$  and  $f_{tie_2} = -0.23p.u.$ . This corresponds to the worst case for the diagnosis filter that the adversary is given the knowledge of the residual generator's parameter  $\bar{N}$  that it tries to minimize the payoff function over  $\mathcal{A}$ . Besides, the noisy system settings have been considered. Figure 3d and Figure 3f demonstrate all the simulation results. In Figure 3d, the static detector becomes totally blind to the occurrence of such an intelligent attack. However, as we can see in Figure 3f, even in the worst case, the diagnosis filter works perfectly well under the noisy system, generate a residual "alert" for the presence of multivariate attacks. This proves the effectiveness and robustness of the proposed diagnosis filter design. To be noted in the end, the pole  $p$  of the diagnosis filter affects its dynamics behavior that it has a faster response but becomes more sensitive to noise when the positive  $p$  is close to zero, while it can be more immune to noise but the response time would increase when the positive  $p$  is larger to be close to 1; See Appendix B 2.3 for the simulation results with different *poles*.

## 6. CONCLUSION AND FURTHER DISCUSSION

*In this article, we investigated the problem of anomaly detection in the power system cyber security with a particular focus on exploiting the dynamics information where tempering multiple measurements data may be possible. Our study showed that a dynamical perspective to the detection task indeed offers powerful diagnosis tools to encounter attack scenarios that may remain stealthy from a static point of view. The effectiveness of*

this result was validated by simulations in the IEEE 39-bus system. Future research directions that we envision include an extension to nonlinear systems, as well as a setting exposed to certain “dynamic” (time-variant) attacks, as opposed to the linear models and stationary attack scenarios studied in this article.

## APPENDIX-A: TECHNICAL PROOFS

### 1.1. Proof of Theorem 4.3

Let us recall that  $\bar{N}V(\alpha) = [N_0FF_b\alpha \quad N_1FF_b\alpha \quad \cdots \quad N_{d_N}FF_b\alpha]$ , and as such, the payoff function of the robust reformulation (18) is  $\mathcal{J}(\bar{N}, \alpha) = \max_i |N_iFF_b\alpha|$  where  $i \in \{0, \dots, d_N\}$ . By introducing an auxiliary variable  $\beta$  in the simplex set  $\mathcal{B} := \{\beta \in \mathbb{R}^{2d_N+2} \mid \beta \geq 0, \mathbf{1}^\top \beta = 1\}$ , one can rewrite  $\mathcal{J}$  as

$$\mathcal{J}(\bar{N}, \alpha) = \max_{\beta \in \mathcal{B}} \sum_{i=0}^{d_N} (\beta_{2i} - \beta_{2i+1}) N_i FF_b \alpha.$$

In this light, the original robust strategy (18) can be equivalently described via

$$\max_{\bar{N} \in \mathcal{N}} \min_{\alpha \in \mathcal{A}} \max_{\beta \in \mathcal{B}} \left\{ \sum_{i=0}^{d_N} (\beta_{2i} - \beta_{2i+1}) N_i FF_b \alpha \right\}.$$

Note that given a fixed  $\bar{N}$  the inner minimax optimization is indeed a bilinear objective in the decision variables and the respective feasible sets  $\mathcal{A}$  and  $\mathcal{B}$  are convex. Since one of the sets,  $\mathcal{B}$ , is also compact, then the zero-duality gap holds. Therefore, interchanging the optimization over  $\alpha \in \mathcal{A}$  and  $\beta \in \mathcal{B}$  yields

$$\gamma^* = \max_{\bar{N} \in \mathcal{N}, \beta \in \mathcal{B}} \left\{ \min_{\alpha \in \mathcal{A}} \sum_{i=0}^{d_N} (\beta_{2i} - \beta_{2i+1}) N_i FF_b \alpha \right\}. \quad (20)$$

The inner minimization of (20) is a (feasible) linear program. We can use the duality again. To this end, let us assume that the decision variables  $\bar{N}$  and  $\beta$  are fixed and consider the Lagrangian function

$$\mathcal{L}(\alpha; \lambda) = b^\top \lambda + \left( \sum_{i=0}^{d_N} (\beta_{2i} - \beta_{2i+1}) N_i FF_b - \lambda^\top A \right) \alpha, \quad (21)$$

where optimizing over an unconstrained variable  $\alpha$  leads to

$$\min_{\alpha} \mathcal{L}(\alpha; \lambda) = \begin{cases} b^\top \lambda & \text{if } \begin{cases} \sum_{i=0}^{d_N} (\beta_{2i} - \beta_{2i+1}) N_i FF_b = \lambda^\top A \\ \lambda \geq 0 \end{cases} \\ -\infty & \text{otherwise,} \end{cases}$$

Using the above characterization as the most inner optimization program in (20) leads to

$$\begin{aligned} \max_{\lambda} \quad & b^\top \lambda \\ \text{s.t.} \quad & \sum_{i=0}^{d_N} (\beta_{2i} - \beta_{2i+1}) N_i FF_b = \lambda^\top A, \\ & \lambda \geq 0. \end{aligned} \quad (22)$$

It then suffices to combine maximizing over the auxiliary variable  $\lambda$  together with the variables  $\bar{N}$  and  $\beta$  to arrive at the main result in (19).

## APPENDIX-B: SYSTEM PARAMETERS AND MORE SIMULATIONS

## 2.1. Dynamic Feedback Controller Modeling

Consider a dynamical system (e.g., the electrical power system studied in Section 3). Suppose the control signal is implemented as a dynamic feedback controller described by the discrete-time dynamics

$$\begin{cases} X_c[k+1] = A_c X_c[k] + B_c Y[k], \\ u[k] = C_c X_c[k] + D_c Y[k], \end{cases} \quad (23)$$

where the input is the dynamical system measurements  $Y[\cdot]$ , the output the control signal  $u[\cdot]$ , and the internal state of the controller is denoted by  $X_c \in \mathbb{R}^{n_c}$ . When an attack occurs on the measurements, it affects the dynamics of the controller and consequently the involved physical system. To study the control dynamics together with the original dynamical system, one can augment the states of the system (3) together with the controller's as  $\hat{X} := [X^\top X_c^\top]^\top$ . Assuming that the control signal can also be measured, one can also introduce an augmented measurement signals as  $\hat{Y} = [Y^\top u^\top]^\top$ . Following this procedure, the dynamics of the closed-loop system is described by

$$\begin{cases} \hat{X}[k+1] = \hat{A}_{cl} \hat{X}[k] + \hat{B}_d d[k] + \hat{B}_f f[k], \\ \hat{Y}[k] = \hat{C} \hat{X}[k] + \hat{D}_f f[k]. \end{cases} \quad (24)$$

where the involved matrices are defined as

$$\begin{aligned} \hat{A}_{cl} &:= \begin{bmatrix} A_x + B_u D_c C & B_u C_c \\ B_c C & A_c \end{bmatrix}, \quad \hat{B}_d := \begin{bmatrix} B_d \\ 0 \end{bmatrix}, \quad \hat{B}_f := \begin{bmatrix} B_u D_c D_f \\ B_c D_f \end{bmatrix}, \\ \hat{C} &:= \begin{bmatrix} C & 0 \\ D_c C & C_c \end{bmatrix}, \quad \hat{D}_f := \begin{bmatrix} D_f \\ D_c D_f \end{bmatrix}. \end{aligned}$$

In this view, the augmented system (24) shares the same structure as (4) studied in the main part of the article for the case of static feedback controller.

## 2.2. AGC System Parameters of the Three-area 39-bus System

We take the matrices description of Area 1 in the three-area 39-bus system of Figure 2 in the main part of the article as an instance,

$$B_{1,d} = \begin{bmatrix} 0 & 0 & -\frac{1}{2H_1} & 0 & 0 & 0 \end{bmatrix}^\top,$$

$$A_{11} = \begin{bmatrix} 0 & 0 & T_{12} & 0 & 0 & 0 \\ 0 & 0 & T_{13} & 0 & 0 & 0 \\ -\frac{1}{2H_1} & -\frac{1}{2H_1} & -\frac{D_1}{2H_1} & \frac{1}{2H_1} & \frac{1}{2H_1} & 0 \\ 0 & 0 & -\frac{1}{T_{ch1,1} S_{1,1}} & -\frac{1}{T_{ch1,1}} & 0 & \frac{\phi_{1,1}}{T_{ch1,1}} \\ 0 & 0 & -\frac{1}{T_{ch1,2} S_{1,2}} & 0 & -\frac{1}{T_{ch1,2}} & \frac{\phi_{1,2}}{T_{ch1,2}} \\ -K_{I_1} & -K_{I_1} & -K_{I_1} B_1 & 0 & 0 & 0 \end{bmatrix}.$$

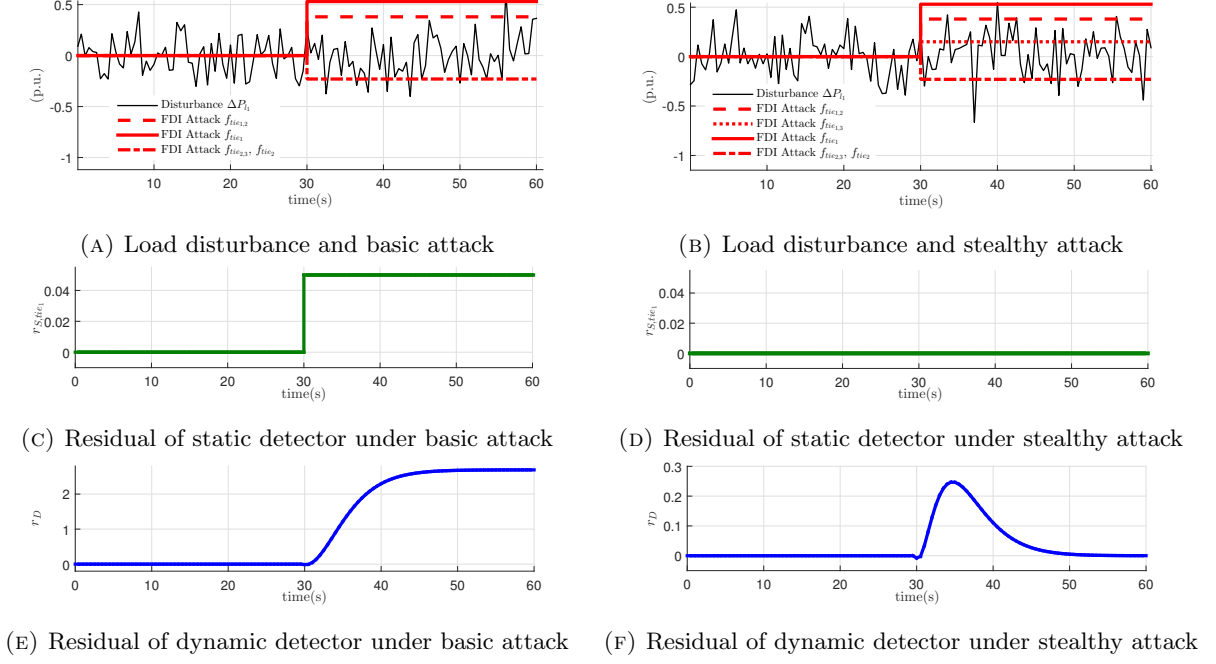


FIGURE 4. Static detector in (2) versus dynamic detector (diagnosis filter) from Corollary IV.4 under basic and stealthy attacks.

As we have assumed a measurement model with high redundancy, the matrix  $C_i$  for Area 1 becomes

$$C_1 = \begin{bmatrix} 1 & 0 & 0 & 0 & 0 & 0 \\ 0 & 1 & 0 & 0 & 0 & 0 \\ 0 & 0 & 1 & 0 & 0 & 0 \\ 0 & 0 & 0 & 1 & 0 & 0 \\ 0 & 0 & 0 & 0 & 1 & 0 \\ 0 & 0 & 0 & 0 & 0 & 1 \\ 1 & 1 & 0 & 0 & 0 & 0 \\ 0 & 0 & 0 & 1 & 1 & 0 \end{bmatrix}^T.$$

In Area 1, the vulnerable measurements to cyber attacks are the ones of tie-line power flows  $\Delta P_{tie1,2}$ ,  $\Delta P_{tie1,3}$  and  $\Delta P_{tie1}$ . Thus the AGC signal  $\Delta P_{agc1}$  would be corrupted into

$$\Delta \dot{P}_{agc1} = -k_1(B_1 \Delta \omega_1 + \Delta P_{tie1,2} + f_{tie1,2} + \Delta P_{tie1,3} + f_{tie1,3}).$$

Then the parameters regarding multivariate attacks are

$$f_1 = \begin{bmatrix} f_{tie1,2} & f_{tie1,3} & f_{tie1} \end{bmatrix}^T,$$

$$D_{1,f} = \begin{bmatrix} 1 & 0 & 0 & 0 & 0 & 0 & 0 & 0 \\ 0 & 1 & 0 & 0 & 0 & 0 & 0 & 0 \\ 0 & 0 & 0 & 0 & 0 & 0 & 1 & 0 \end{bmatrix}^T,$$

$$B_{1,f} = \begin{bmatrix} 0 & 0 & 0 & 0 & 0 & -k_1 \\ 0 & 0 & 0 & 0 & 0 & -k_1 \\ 0 & 0 & 0 & 0 & 0 & 0 \end{bmatrix}^T.$$

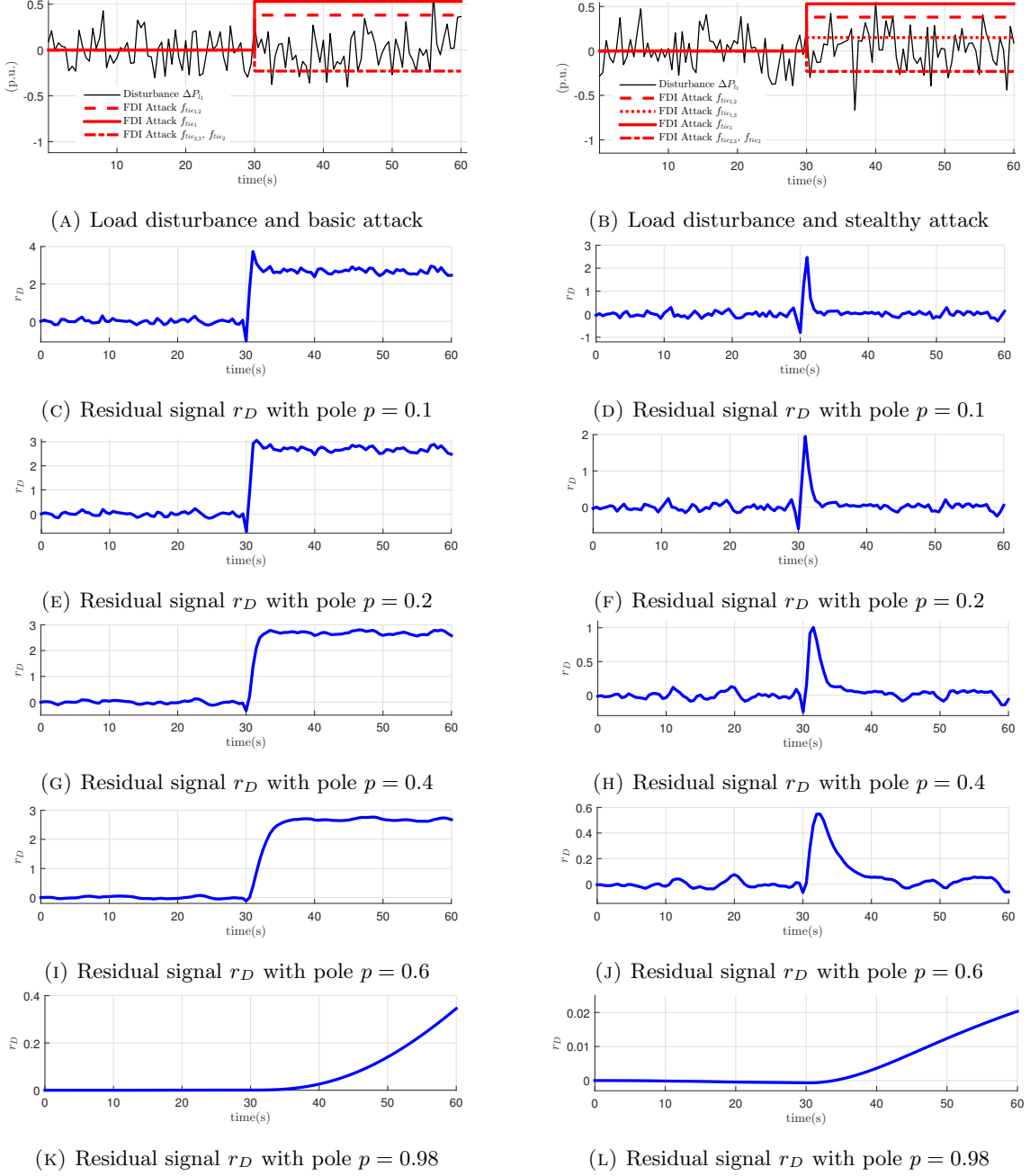


FIGURE 5. Results of dynamic detector (diagnosis filter) with different *poles* under basic and stealthy attacks.

### 2.3. Simulation Results of Ideal Scenarios and Diagnosis Filter with Different *poles*

In the main part of the article, the simulation results of both detectors under noisy systems have been illustrated in Figure 3. Next in Figure 4 we present the simulation results of detector residuals  $r_S$ ,  $r_D$  under ideal scenarios where there is no noise in the process and measurements.

In Figure 5 we present the simulation results of residual signal  $r_D$  of the proposed diagnosis filter under different poles ( $p = 0.1, 0.2, 0.4, 0.6, 0.98$  respectively.)



## APPENDIX-C: DIAGNOSIS FILTER WITH NON-ZERO STEADY-STATE RESIDUAL

The diagnosis filter design proposed in Subsection 4.2 does not enforce a non-zero steady-state residual under multivariate attacks. In fact, as Figure 4f shows, the residual signal  $r_D$  of the diagnosis filter under stealthy attacks may become zero, in this particular case after  $k = 50$  sec. In order to design a diagnosis filter with non-zero steady-state residual “alerts” when multivariate attacks occur, one can modify Lemma 4.2 in the following fashion.

**Lemma 3.1** (Non-zero steady-state residual characterization). *For the polynomial matrices  $H(q)$ ,  $N(q)$  and  $F(q)$ , the family of dynamic residual generators in (16) but with non-zero steady-state residual under multivariate attacks can be characterized by the algebraic relations*

$$\begin{cases} (I) & \bar{N}\bar{H} = 0, \\ (II) & |\bar{N}\bar{F}\alpha| > 0, \quad \text{for all } \alpha \in \mathcal{A}, \end{cases} \quad (25)$$

where

$$\bar{F} := \begin{bmatrix} FF_b & FF_b & \cdots & FF_b \end{bmatrix}^\top.$$

and  $\bar{N}$ ,  $\bar{H}$  are the same to the ones defined in Lemma 4.2.

*Proof.* Recall that  $N(q)H(q) = \bar{N}\bar{H}[I, qI, \dots, q^{d_{N+1}}I]^\top$ . Thus if  $\bar{N}\bar{H} = 0$ , the diagnosis filter becomes  $r_D[k] = -a(q)^{-1}N(q)f[k]$ . Note the steady-state value of the filter residual under attacks would be  $-a(q)^{-1}N(q)F(q)f|_{q=1}$ . Thus for the multivariate attack with  $\alpha$ , the steady-state value of the filter residual is  $-a(1)^{-1}N(1)F(1)F_b\alpha$ . The proof concludes by noting that  $N(1)F(1)F_b\alpha = \bar{N}\bar{F}\alpha$ .  $\square$

Similarly, we can have a robust optimization for the diagnosis filter design with the objective function  $\mathcal{J}(\bar{N}, \alpha) := |\bar{N}\bar{F}\alpha|$ , representing the absolute steady state gain from the attacks to the filter residual. In particular, the aim is to find filter parameters  $\bar{N}^*$  such that  $\mathcal{J}(\bar{N}^*, \alpha) > 0$  for all  $\alpha \in \mathcal{A}$ . To this end, we define

$$\mu^* := \max_{\bar{N} \in \mathcal{N}} \min_{\alpha \in \mathcal{A}} \left\{ \mathcal{J}(\bar{N}, \alpha) := |\bar{N}\bar{F}\alpha| \right\}. \quad (26)$$

The next result is similar to Theorem 4.3 but with the new objective function (26).

**Theorem 3.2** (Reformulation of non-zero steady state gain). *Consider the symmetric feasible set of the filter coefficients  $\mathcal{N}$  as defined in (17). The robust optimization (26) can be equivalently described via the linear optimization program*

$$\begin{aligned} \mu^* &= \max_{\bar{N}, z} b^\top z \\ \text{s.t.} & \quad \bar{N}\bar{F} = z^\top A, \\ & \quad \bar{N} \in \mathcal{N}, \quad z \geq 0. \end{aligned} \quad (27)$$

*Proof.* For a given  $\bar{N} \in \mathcal{N}$ , the inner minimization of (26) can be equivalently translated as

$$\begin{aligned} \min_{\alpha \in \mathcal{A}} & \quad r \\ \text{s.t.} & \quad \bar{N}\bar{F}\alpha - r \leq 0, \\ & \quad -\bar{N}\bar{F}\alpha - r \leq 0. \end{aligned}$$

The Lagrangian of the inner minimization over the variable  $\alpha$  reads as

$$\mathcal{L}(\alpha, r, v_1, v_2, z) = b^\top z + ((v_1 - v_2)\bar{N}\bar{F} - z^\top A)\alpha + (1 - v_1 - v_2)r.$$

Optimizing over the variable  $\alpha \in \mathcal{A}$  yields the dual function

$$\min_{\alpha \in \mathcal{A}} \mathcal{L}(\alpha, r, v_1, v_2, z) = \begin{cases} b^\top z & \text{if } (v_1 - v_2)\bar{N}\bar{F} = z^\top A, v_1 + v_2 \leq 1, \\ & v_1 \geq 0, v_2 \geq 0, z \geq 0, \\ -\infty & \text{otherwise.} \end{cases}$$

Then, combining maximization over the auxiliary variable  $z$  together with  $\bar{N}$  and  $v_1, v_2$  arrives at the optimization program

$$\begin{aligned} \mu^* &= \max_{\bar{N}, v_1, v_2, z} b^\top z \\ \text{s.t.} \quad & (v_1 - v_2)\bar{N}\bar{F} = z^\top A, \\ & v_1 + v_2 \leq 1, v_1 \geq 0, v_2 \geq 0, \\ & \bar{N} \in \mathcal{N}, z \in \mathbb{R}^{n_b}, z \geq 0. \end{aligned} \tag{28}$$

Note that the actual program (27) is a restriction of (28) where the variables  $v_1, v_2$  are restricted to  $v_1 = 1$  and  $v_2 = 0$ . In the rest of the proof we show that this restriction is indeed without loss of generality. To this end, suppose the tuple  $(v_1^*, v_2^*, \bar{N}^*, z^*)$  is an optimal solution to the program (28). Note that the optimal variables  $v_1^*$  and  $v_2^*$  may satisfy one of the following three properties:

- (i)  $v_1^* = v_2^*$ : In this case,  $z^* = 0$ , and therefore the optimal value  $\mu^* = 0$ . This optimal solution can be trivially achieved in the program (27) by setting  $\bar{N} = 0$ .
- (ii)  $v_1^* > v_2^*$ : Observe that the tuple  $(v_1' = 1, v_2' = 0, \bar{N}' = \bar{N}^*, z' = z^*/(v_1^* - v_2^*))$  is a feasible solution with the objective value  $b^\top z^*/(v_1^* - v_2^*)$ . Since  $b^\top z^* \geq 0$  by optimality assumption and  $v_1^* - v_2^* \in (0, 1]$ , then this feasible solution has a possibly higher optimal value, and therefore  $v_1^* - v_2^* = 1$ . That is,  $v_1^* = 1$  and  $v_2^* = 0$ .
- (iii)  $v_1^* < v_2^*$ : Following similar steps as the previous case together with the symmetric property of the feasible set  $\mathcal{N}$ , one can show that the optimal value of the program (28) also coincides with the restricted version in (27).

this concludes the proof. □

## REFERENCES

- [1] A. ABUR AND A. G. EXPOSITO, *Power system state estimation: theory and implementation*, CRC press, 2004.
- [2] A. AMELI, A. HOOSHYAR, E. EL-SAADANY, AND A. YOUSSEF, *Attack detection and identification for automatic generation control systems*, IEEE Transactions on Power Systems, (2018), p. 1.
- [3] A. ASHOK, M. GOVINDARASU, AND V. AJJARAPU, *Online detection of stealthy false data injection attacks in power system state estimation*, IEEE Transactions on Smart Grid, 9 (2018), pp. 1636–1646.
- [4] H. BEVRANI, *Robust Power System Frequency Control*, Power Electronics and Power Systems, Springer, 2008.
- [5] C. CHEN, K. ZHANG, K. YUAN, L. ZHU, AND M. QIAN, *Novel detection scheme design considering cyber attacks on load frequency control*, IEEE Transactions on Industrial Informatics, 14 (2018), pp. 1932–1941.
- [6] T. M. CHEN AND S. ABU-NIMEH, *Lessons from sturnet*, Computer, 44 (2011), pp. 91–93.
- [7] C. CYBERSECURITY, *Framework for improving critical infrastructure cybersecurity version 1.1*, tech. rep., National Institute of Standards and Technology, Apr. 2018.
- [8] R. DENG AND H. LIANG, *False data injection attacks with limited susceptance information and new countermeasures in smart grid*, IEEE Transactions on Industrial Informatics, (2018), p. 1.
- [9] S. X. DING, *Model-based fault diagnosis techniques: design schemes, algorithms, and tools*, Springer Science & Business Media, 2008.
- [10] P. M. ESFAHANI AND J. LYGEROS, *A tractable fault detection and isolation approach for nonlinear systems with probabilistic performance*, IEEE Transactions on Automatic Control, 61 (2016), pp. 633–647.
- [11] S. GORMAN, *Electricity grid in US penetrated by spies*, The Wall Street Journal, 8 (2009).

- [12] G. HUG AND J. A. GIAMPAPA, *Vulnerability assessment of AC state estimation with respect to false data injection cyber-attacks*, IEEE Transactions on Smart Grid, 3 (2012), pp. 1362–1370.
- [13] D. KIRSCHEN AND F. BOUFFARD, *Keeping the lights on and the information flowing*, IEEE Power and Energy Magazine, 7 (2009), pp. 50–60.
- [14] S. LI, Y. YILMAZ, AND X. WANG, *Quickest detection of false data injection attack in wide-area smart grids*, IEEE Transactions on Smart Grid, 6 (2015), pp. 2725–2735.
- [15] G. LIANG, S. R. WELLER, J. ZHAO, F. LUO, AND Z. Y. DONG, *The 2015 Ukraine blackout: Implications for false data injection attacks*, IEEE Transactions on Power Systems, 32 (2017), pp. 3317–3318.
- [16] J. LIANG, L. SANKAR, AND O. KOSUT, *Vulnerability analysis and consequences of false data injection attack on power system state estimation*, IEEE Transactions on Power Systems, 31 (2016), pp. 3864–3872.
- [17] L. LIU, M. ESMALIFALAK, Q. DING, V. A. EMESIH, AND Z. HAN, *Detecting false data injection attacks on power grid by sparse optimization*, IEEE Transactions on Smart Grid, 5 (2014), pp. 612–621.
- [18] Y. LIU, P. NING, AND M. K. REITER, *False data injection attacks against state estimation in electric power grids*, in Proc. of the 16th ACM Conf. on Computer and Comm. Security, New York, 2009, pp. 21–32.
- [19] M. A. MASSOUMNIA, G. C. VERGHESE, AND A. S. WILLSKY, *Failure detection and identification*, IEEE Transactions on Automatic Control, 34 (1989), pp. 316–321.
- [20] M. NYBERG AND E. FRISK, *Residual generation for fault diagnosis of systems described by linear differential-algebraic equations*, IEEE Transactions on Automatic Control, 51 (2006), pp. 1995–2000.
- [21] K. OGATA, *Discrete-time Control Systems (2Nd Ed.)*, Prentice-Hall, Inc., Upper Saddle River, NJ, USA, 1995.
- [22] E. RAKHSHANI, D. REMON, A. M. CANTARELLAS, J. M. GARCIA, AND P. RODRIGUEZ, *Virtual synchronous power strategy for multiple hvdc interconnections of multi-area ac power systems*, IEEE Transactions on Power Systems, 32 (2017), pp. 1665–1677.
- [23] A. TEIXEIRA, S. AMIN, H. SANDBERG, K. H. JOHANSSON, AND S. S. SASTRY, *Cyber security analysis of state estimators in electric power systems*, in IEEE Conference on Decision and Control, 2010.
- [24] E. E. TINIOU, P. MOHAJERIN ESFAHANI, AND J. LYGEROS, *Fault detection with discrete-time measurements: An application for the cyber security of power networks*, in IEEE Conference on Decision and Control, 2013.
- [25] J. ZHAO, L. MILI, AND M. WANG, *A generalized false data injection attacks against power system nonlinear state estimator and countermeasures*, IEEE Transactions on Power Systems, (2018), p. 1.